

Lattice QCD results on cumulant ratios at freeze-out

Frithjof Karsch

Fakultät für Physik, Universität Bielefeld, D-33615 Bielefeld, Germany;

Physics Department, Brookhaven National Laboratory, Upton, NY 11973, USA

E-mail: karsch@bnl.gov

Abstract. Ratios of cumulants of net proton-number fluctuations measured by the STAR Collaboration show strong deviations from a skellam distribution, which should describe thermal properties of cumulant ratios, if proton-number fluctuations are generated in equilibrium and a hadron resonance gas (HRG) model would provide a suitable description of thermodynamics at the freeze-out temperature. We present some results on 6th order cumulants entering the calculation of the QCD equation of state at non-zero values of the baryon chemical potential (μ_B) and discuss limitations on the applicability of HRG thermodynamics deduced from a comparison between QCD and HRG model calculations of cumulants of conserved charge fluctuations. We show that basic features of the μ_B -dependence of skewness and kurtosis ratios of net proton-number fluctuations measured by the STAR Collaboration resemble those expected from a $\mathcal{O}(\mu_B^2)$ QCD calculation of the corresponding net baryon-number cumulant ratios.

1. Introduction

A major goal in current experimental and theoretical studies of the thermodynamics of strong interaction matter is the exploration of its phase diagram. The hope is to find evidence for the existence of a second order phase transition point – the chiral critical point (CCP) – located at some value of the chemical potential, μ_B^{crit} [1]. This would be the starting point for a line of first order phase transitions at larger values of the baryon chemical potential μ_B .

At RHIC a dedicated research program – the beam energy scan (BES) – has been established that seeks evidence for the existence and location of the CCP. By varying the beam energy properties of matter in a regime of temperatures (T) up to about three times the transition temperature, $T_{pc} \sim 155$ MeV [2, 3], and baryon chemical potential up to $\mu_B \simeq 3T$ can be probed. It is generally expected that conserved charge fluctuations, which are generated close to, or at the freeze-out temperature, $T_f(\mu_B)$, can provide insight into the existence and location of the CCP. An important prerequisite for such studies, however, is to understand the thermodynamics of hot and dense matter in the crossover region and, in particular, close to freeze-out in QCD.

In the following we will point out the importance of characterizing this regime in terms of QCD rather than hadron resonance gas (HRG) model calculations, which are quite successful in approximating QCD thermodynamics at sufficiently low temperatures, but definitely fail to capture important aspects of QCD thermodynamics visible in conserved charge fluctuations at temperatures $T \gtrsim 160$ MeV.

2. Energy density in the crossover region

At small values of μ_B the QCD transition is not a true phase transition but a smooth transition from the low- T hadronic to the high- T partonic regime. This *crossover transition*

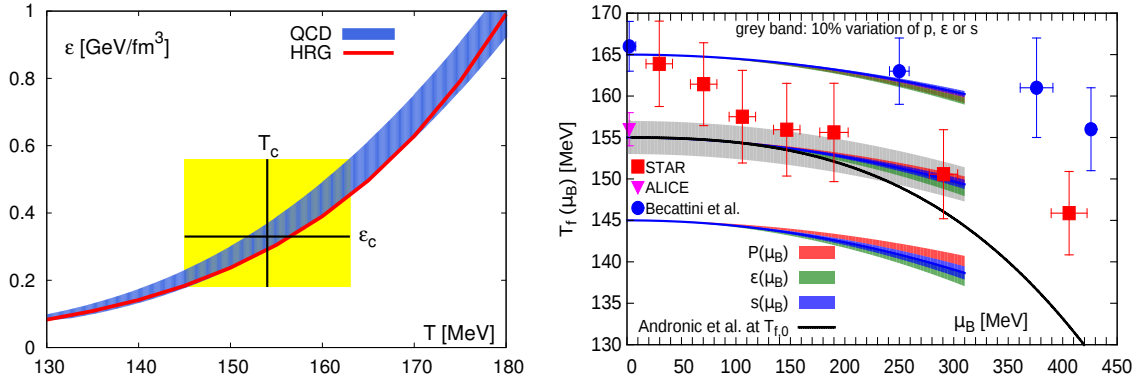


Figure 1. *Left:* Energy density of QCD versus temperature obtained from lattice QCD calculations (band) and HRG model calculations (line). *Right:* Freeze-out temperatures versus baryon chemical potential determined by STAR (boxes) [7] and ALICE (triangle) [8], and hadronization temperatures (circle) determined in Ref. [9]. The bands show lines of constant pressure, energy density and entropy density, respectively. They have been determined from a $\mathcal{O}(\mu_B^2)$ Taylor expansion of the QCD partition function. Also shown is a parametrization of the freeze-out line suggested by Andronic et al. (black line) [10] shifted to $T_f(0) = 155$ MeV.

does not happen at a well defined temperature. However, it can be characterized by pseudo-critical temperatures, i.e. temperatures that reflect characteristic features of e.g. fluctuation observables, which are guaranteed to converge to the true critical temperature in the chiral limit. One such observable is the chiral susceptibility, χ_q , the derivative of the chiral condensate with respect to quark mass. The location of the maximum of χ_q defines a pseudo-critical temperature. This has been obtained in lattice QCD calculations, $T_{pc} = 154(9)$ MeV [3].

In Fig. 1 (left) we show results for the energy density (ϵ) obtained from lattice QCD calculations with physical strange and light quark masses [6]. The temperature range covered by current uncertainties in T_{pc} corresponds to $\epsilon_c = (0.34 \pm 0.16)$ GeV/fm³. Unfortunately, this energy density range is still quite large. In fact, it covers practically all energy scales of interest. While the central value corresponds to the close packing limit of nucleons with a radius $r_n \simeq 0.8$ fm, the lower limit is close to the energy density of nuclear matter ($\epsilon_{nm} \simeq 0.15$ GeV/fm³) and the upper limit is larger than the energy density inside a nucleon ($\epsilon_n \simeq 0.45$ GeV/fm³).

Using the Taylor expansion of the QCD equation of state one can follow lines of constant physics in the T - μ_B plane. In Fig. 1 (right) we show lines of constant pressure (p), energy density (ϵ) and entropy density (s) obtained in order μ_B^2 . Corrections to this are small for $\mu_B/T \leq 2$. The three sets of curves, characterizing the current uncertainty band on T_{pc} , correspond to $\epsilon = 0.2$, 0.35 and 0.56 GeV/fm³. Given the current uncertainties on T_{pc} it is not too surprising that all results on freeze-out parameters ($T_f(\mu_B)$, μ_B) obtained from the analysis of particle yields at the LHC [8] and RHIC [7] and even the rather large hadronization temperatures extracted in Ref. [9] allow to state that "hadronization and freeze-out of hadrons occur close to, or in the QCD crossover region" (see Fig. 1 (right)) even though the temperatures in question are quite different, e.g. ranging from 155 MeV to 165 MeV at $\mu_B = 0$. They refer to environments, in which hadronization and freeze-out may take place, that are quite different, e.g. the energy and entropy density may differ by a factor 2. Lattice QCD calculations provide a wealth of other observables, e.g. higher order cumulants of conserved charge fluctuations, that are sensitive to the changes in physical properties of hot and dense matter that occur in this temperature interval. Understanding these changes also is of importance for our understanding of freeze-out conditions determined with the BES at RHIC as well as at the LHC.

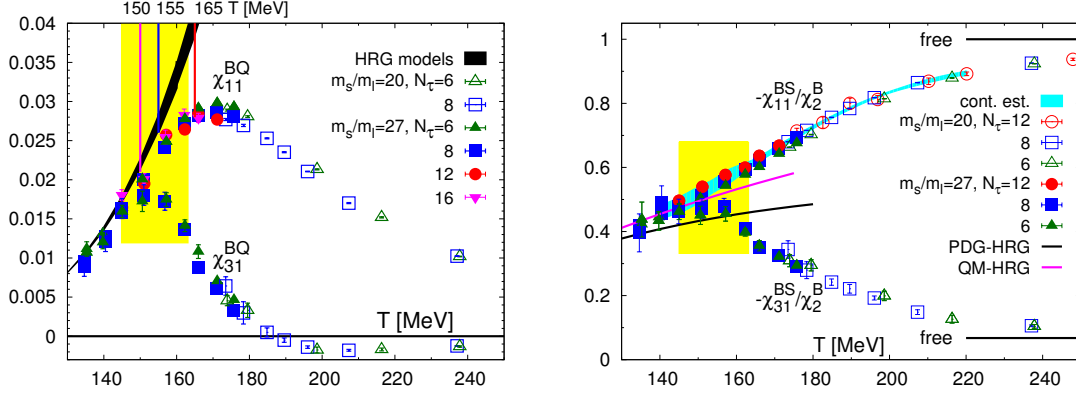


Figure 2. *Left:* Correlation between net baryon-number and net electric charge fluctuations (χ_{11}^{BQ}) versus temperature and the third moment of net baryon-number and net electric charge fluctuations (χ_{31}^{BQ}). The yellow band shows the crossover region defined by the uncertainty of the pseudo-critical temperature $T_{pc} = (154 \pm 9)$ MeV. *Right:* same as on the left but for correlations between net baryon-number and net strangeness fluctuations. These cumulants have been normalized with the quadratic fluctuations of net baryon-number.

3. Cumulants of conserved charge fluctuations

At $\mu_B = 0$ the energy density calculated in QCD as well as HRG models shown in Fig. 1 (left) varies smoothly as function of temperature when traversing the crossover region. Even quantitatively the latter is in quite good agreement with QCD calculations, although it has been pointed out that the QCD energy density is systematically larger, which may be taken as evidence for additional hadronic degrees of freedom contributing to bulk thermodynamics close to T_{pc} [4, 5]. Nonetheless, HRG model calculations seem to describe bulk thermodynamics quite well even at temperatures as large as $T \sim 180$ MeV. In fact, the situation is similar even for the specific heat [6]. Does this mean that the strongly interacting medium can be described in terms of hadronic degrees of freedom in the entire crossover region and even above?

Conserved charge fluctuations and correlations between them provide plenty of evidence that thermodynamics described in terms of hadronic degrees of freedom breaks down close to T_{pc} . In particular, higher order cumulants are quite different from conventional HRG model calculations. We show in Fig. 2 two examples of this. The left hand figure shows second and fourth order cumulants of net baryon-number and net electric charge fluctuations,

$$\chi_{11}^{BQ} = \left. \frac{\partial^2 p / T^4}{\partial \hat{\mu}_B \partial \hat{\mu}_Q} \right|_{\vec{\mu}=0}, \quad \chi_{31}^{BQ} = \left. \frac{\partial^4 p / T^4}{\partial \hat{\mu}_B^3 \partial \hat{\mu}_Q} \right|_{\vec{\mu}=0}, \quad (1)$$

with $\hat{\mu}_X \equiv \mu_X / T$ and $\vec{\mu} = (\mu_B, \mu_Q, \mu_S)$. In the infinite temperature, ideal quark gas limit the net electric charge of 3-flavor QCD vanishes. Thus χ_{11}^{BQ} and χ_{31}^{BQ} will both approach zero while these correlations will keep increasing exponentially in HRG model calculations with point-like, non interacting hadrons.

At low temperature all hadronic degrees of freedom will either carry baryon number $B = 0$ or $B = \pm 1$. HRG model calculations thus give $\chi_{11}^{BQ} = \chi_{31}^{BQ}$. It is obvious from Fig. 2 (left) that this relation no longer holds for $T \gtrsim 150$ MeV. Also χ_{11}^{BQ} starts deviating from HRG model calculations at $T \gtrsim 155$ MeV. A similar pattern is found for second and fourth order cumulants of net baryon-number and net strangeness correlations shown in Fig. 2 (right). Various other combinations of 2nd and 4th order cumulants have been constructed that make it apparent that HRG models with point-like non-interacting hadrons are not suitable for describing QCD

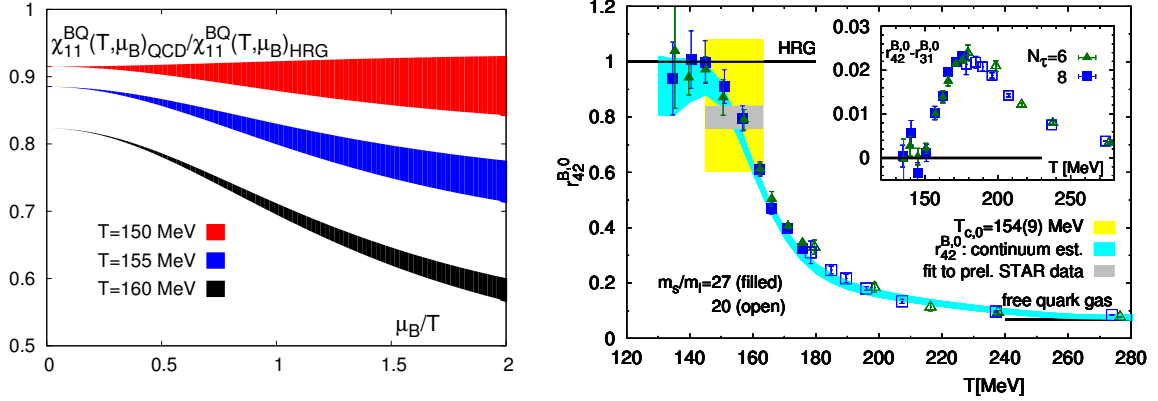


Figure 3. Correlations between net baryon-number and net electric charge as function of μ_B/T for three values of the temperature. Results from a QCD calculation at next-to-leading order Taylor expansion are normalized to a HRG model calculations truncated at the same order.

thermodynamics at temperatures $T \gtrsim T_{pc}$ [11]. In fact, this also has been verified for net baryon-number and net charm correlations [12] which strongly suggests that also the thermodynamics of open charm baryons cannot be described by HRG models above T_{pc} .

A consequence of the early deviation of 4^{th} order cumulants from corresponding HRG calculations also is that differences between QCD and HRG calculations increase with increasing value of the chemical potential and will show up already in 2^{nd} order cumulants. This is shown in Fig. 3 (left) for the correlation between net baryon-number and net electric charge evaluated up to $\mathcal{O}(\mu_B^2)$,

$$\chi_{11}^{BQ}(T, \mu_B) = \chi_{11}^{BQ} + \frac{1}{2} \chi_{31}^{BQ} \mu_B^2. \quad (2)$$

Obviously QCD and HRG calculations differ significantly at $\mu_B/T = 2$ already for $T \gtrsim 155$ MeV.

4. Taylor expansions for skewness and kurtosis ratios

In HRG models with point-like non-interacting hadrons the distribution of net baryon number fluctuations is given by a skellam distribution. This leads to quite simple properties of higher order cumulants. In particular, the skewness ratio $S_B \sigma_B^3 / M_B$ and the kurtosis ratio $\kappa_B \sigma_B^2$ should both be equal to unity at all values of μ_B . However, as discussed in the previous section this cannot be expected to hold in QCD at temperatures above T_{pc} where cumulants start to deviate significantly from HRG model calculations. The distribution of net baryon number fluctuations thus is e.g. not a simple skellam distribution. QCD calculations of the skewness and kurtosis ratios yield

$$\frac{S_B \sigma_B^3}{M_B} = \frac{\chi_3^B(T, \mu_B)}{\chi_1^B(T, \mu_B)} = \frac{\chi_4^B + s_1 \chi_{31}^{BS} + q_1 \chi_{31}^{BQ}}{\chi_2^B + s_1 \chi_{11}^{BS} + q_1 \chi_{11}^{BQ}} + \mathcal{O}(\mu_B^2) \equiv r_{31}^{B,0} + r_{31}^{B,2} \mu_B^2 + \mathcal{O}(\mu_B^4) \quad (3)$$

$$\kappa_B \sigma_B^2 = \frac{\chi_4^B(T, \mu_B)}{\chi_2^B(T, \mu_B)} = \frac{\chi_4^B}{\chi_2^B} + \mathcal{O}(\mu_B^2) \equiv r_{42}^{B,0} + r_{42}^{B,2} \mu_B^2 + \mathcal{O}(\mu_B^4), \quad (4)$$

with s_1 and q_1 denoting the leading order expansion coefficients of μ_S and μ_Q in terms of μ_B that result from imposing the strangeness neutrality constraint $M_S = 0$ and a fixed electric charge to baryon number ratio, $M_Q/M_B = 0.4$. Results for the leading order expansion coefficients, defined in Eqs. 3 and 4, are shown in Fig. 3 (right). While at $T \simeq 150$ MeV the kurtosis ratio at $\mu_B = 0$ is still close to unity, $\kappa_B \sigma_B^2 \simeq 0.9$, it strongly deviates from unity for $T \simeq 160$ MeV,

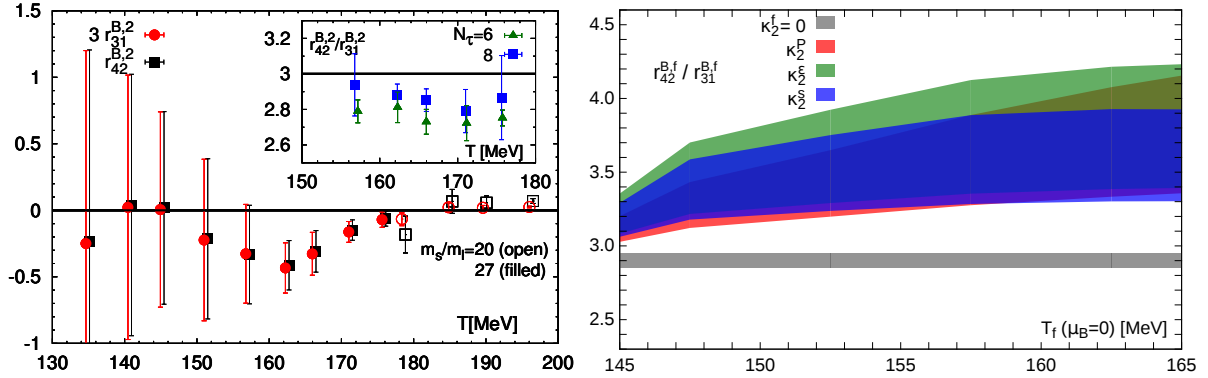


Figure 4. *Left:* The next-to-leading order (NLO) expansion coefficients of the skewness and kurtosis ratios at fixed temperature as introduced in Eqs. 3 and 4. *Right:* The ratio of the NLO expansion coefficients taking into account also a NLO expansion in terms of temperature along the line of constant pressure, energy density or entropy density, respectively.

giving $\kappa_B \sigma_B^2 \simeq 0.6$. In view of these differences it also is not obvious that the skewness and kurtosis ratios will still coincide in a QCD calculation. However, as can be seen from Eqs. 3 and 4 at $\mu_B = 0$ the leading order results will always be identical, if $\mu_Q = \mu_S = 0$, irrespective of the size of deviation from the skellam limit. For non-zero μ_Q and μ_S the skewness and kurtosis ratios will differ. Nonetheless, as can be seen from the insertion in Fig. 3 (right) this difference is small for all temperatures of interest. QCD thus predicts that the skewness and kurtosis ratios will approach each other in the limit $\mu_B \rightarrow 0$. This, however, changes for $|\mu_B| \neq 0$.

At next-to-leading order (NLO) the expansion coefficients $r_{31}^{B,2}$ and $r_{42}^{B,2}$ need to be calculated. This is computationally difficult, because 6th order cumulants need to be evaluated. Current results for $r_{31}^{B,2}$ and $r_{42}^{B,2}$ are shown in Fig. 4 (left). Although errors are still large, it is apparent that these expansion coefficients are negative for $150 \text{ MeV} \lesssim T \lesssim 175 \text{ MeV}$ and that $r_{42}^{B,2}$ is about three times larger than $r_{31}^{B,2}$. This has been reported by us earlier [13]. It thus is expected that the skewness and kurtosis ratios, which are almost identical at $\mu_B = 0$, will start to differ for $\mu_B > 0$. As the expansion coefficients are negative, $\kappa_B \sigma_B^2$ will drop faster than $S_B \sigma_B^3 / M_B$.

An additional subtlety in the analysis of the μ_B -dependence of the skewness and kurtosis ratios is that these need to be evaluated at a (freeze-out) temperature that changes with μ_B . This requires an additional Taylor expansion of the ratios introduced in Eqs. 3 and 4. Assuming that freeze-out happens along a line of constant physics described either by constant pressure, energy density or entropy density, i.e. the lines shown in Fig. 1, these contributions can be evaluated using the Taylor expansion of the pressure [16], changing $r_{nm}^{B,2}$ to $r_{nm}^{B,f}$. It turns out that the additional contributions increase the ratio $r_{42}^{B,f}/r_{31}^{B,f}$ somewhat as shown in Fig. 4 (right).

5. The STAR data on net proton-number skewness and kurtosis ratios

The STAR collaboration has measured the skewness ratio $S_P \sigma_P^3 / M_P$ and kurtosis ratio $\kappa_P \sigma_P^2$ of net proton-number fluctuations [14, 15]. Obviously these cumulant ratios cannot directly be compared to QCD results on net baryon-number fluctuations. Already the strong sensitivity on the transverse momentum range used in the analysis, which is clearly visible in the data published so far by the STAR Collaboration (Fig. 5 (left) and (right), respectively), emphasizes that there is need for better understanding of various effects that enter the experimental analysis of higher order cumulants. Nonetheless, it is striking that the published as well as the new preliminary data on skewness and kurtosis ratios resemble all the features we expect to show up

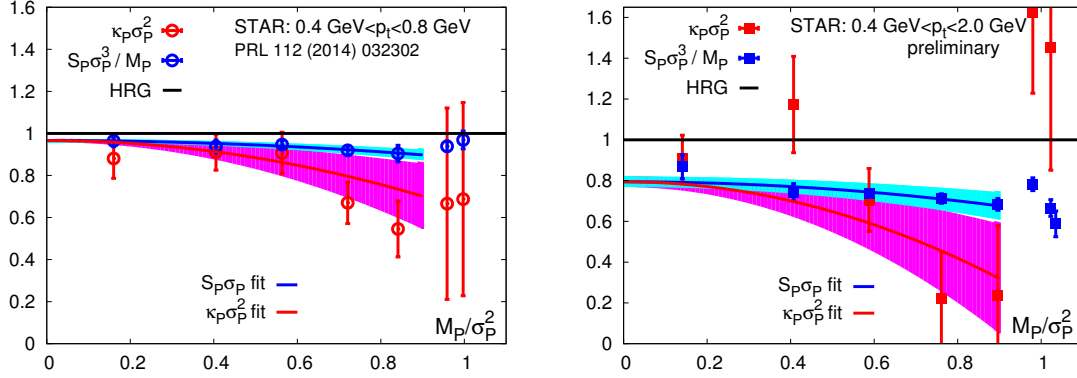


Figure 5. Skewness and kurtosis ratios of net proton-number fluctuations measured by the STAR collaboration in transverse momentum intervals $0.4 \text{ GeV} < p_t < 0.8 \text{ GeV}$ (left) and $0.4 \text{ GeV} < p_t < 2.0 \text{ GeV}$ (right), respectively. Data are plotted versus the ratio of mean (M_P) over variance (σ_P^2) of the net proton-number distribution, which also is measured at various beam energies. Curves show combined fits to the data for $M_P/\sigma_P^2 < 0.9$ or equivalently $\sqrt{s_{NN}} \leq 19.6 \text{ GeV/fm}^3$. They are constraint by demanding $S_P \sigma_P^3 / M_P = \kappa_P \sigma_P^2$ at $M_P/\sigma_P^2 = 0$.

in equilibrium thermodynamics of QCD. The ratios (i) are smaller than unity, (ii) they seem to coincide in the limit $\mu_B \rightarrow 0$, (iii) they have a negative slope with increasing μ_B and (iv) the kurtosis ratio drops faster than the skewness ratio. In fact, a combined quadratic fit to these ratios, performed for all data obtained at beam energies $\sqrt{s_{NN}} \geq 19.6 \text{ GeV/fm}^3$ and imposing the constraint $r_{42}^{B,0}/r_{31}^{B,0}$, yields for the ratio of slope parameters $r_{42}^{B,f}/r_{31}^{B,f} \sim 4 \pm 2$, which is in good agreement with the NLO QCD result shown in Fig. 4 (left). These fits are shown in Fig. 5.

Acknowledgments

This work has been partially supported through the U.S. Department of Energy under Contract No. de-sc0012704 and within the framework of the Beam Energy Scan Theory (BEST) Topical Collaboration, and the German Bundesministerium für Bildung und Forschung (BMBF) under grant no. 05P15PBCAA.

References

- [1] H. T. Ding, F. Karsch and S. Mukherjee, Int. J. Mod. Phys. E **24**, 1530007 (2015) [arXiv:1504.05274 [hep-lat]].
- [2] Y. Aoki et al., JHEP **0906**, 088 (2009) [arXiv:0903.4155 [hep-lat]].
- [3] A. Bazavov et al., Phys. Rev. D **85**, 054503 (2012) [arXiv:1111.1710 [hep-lat]].
- [4] A. Majumder and B. Muller, Phys. Rev. Lett. **105**, 252002 (2010) [arXiv:1008.1747 [hep-ph]].
- [5] A. Bazavov et al., Phys. Rev. Lett. **113**, 072001 (2014) [arXiv:1404.6511 [hep-lat]].
- [6] A. Bazavov et al. [HotQCD Collaboration], Phys. Rev. D **90**, 094503 (2014) [arXiv:1407.6387 [hep-lat]].
- [7] S. Das [STAR Collaboration], EPJ Web Conf. **90**, 08007 (2015) [arXiv:1412.0499 [nucl-ex]].
- [8] M. Floris, Nucl. Phys. A **931**, 103 (2014) [arXiv:1408.6403 [nucl-ex]].
- [9] F. Becattini, J. Steinheimer, R. Stock and M. Bleicher, arXiv:1605.09694 [nucl-th].
- [10] A. Andronic, P. Braun-Munzinger and J. Stachel, Phys. Lett. B **673**, 142 (2009) Erratum: [Phys. Lett. B **678**, 516 (2009)] [arXiv:0812.1186 [nucl-th]].
- [11] A. Bazavov et al., Phys. Rev. Lett. **111**, 082301 (2013) [arXiv:1304.7220 [hep-lat]].
- [12] A. Bazavov et al., Phys. Lett. B **737**, 210 (2014) [arXiv:1404.4043 [hep-lat]].
- [13] F. Karsch et al., arXiv:1512.06987 [hep-lat].
- [14] M. M. Aggarwal et al. [STAR Collaboration], Phys. Rev. Lett. **105**, 022302 (2010).
- [15] X. Luo [STAR Collaboration], PoS CPOD **2014**, 019 (2015) [arXiv:1503.02558 [nucl-ex]].
- [16] Bielefeld-BNL-CCNU Collaboration, in preparation.